ACS APPLIED MATERIALS & INTERFACES

Research Article

www.acsami.org

Ultraintense Short-Wavelength Emission from ZnO-Sheathed MgO Nanorods Induced by Subwavelength Optical Resonance Cavity Formation: Verification of Previous Hypothesis

Changhyun Jin, Hyunsu Kim, and Chongmu Lee*

Department of Materials Science and Engineering, Inha University, 253 Yonghyun-dong, Nam-gu, Incheon 402-751, Republic of Korea

ABSTRACT: A recent paper reported that intense emissions with a range of wavelengths over a wide spectral range, from ultraviolet to infrared light, might be possible by sheathing MgO nanorods with a semiconducting material with an optimal sheath thickness. In addition, the paper hypothesized that an ultraintense short-wavelength emission could be obtained by sheathing MgO nanorods with a ~17 nm ZnO thin film in the paper. In this study, we found that the intensity ratio of the near-band edge emission to the deep level emission (I_{NBE}/I_{DL}) of the MgO-core/ZnO-shell nanorods with a mean shell layer thickness of 17 nm was as high as ~30, whereas the I_{NBE}/I_{DL} ratio of the bare-MgO nanorods was 0. This near-band edge emission intensity enhancement by sheathing the MgO nanorods with ZnO is by far more significant than that by sheathing the ZnO nanorods with other materials including MgO. This is because subwavelength optical resonance cavities form in the MgO-core/ZnO-shell nanorods with faceted surfaces, whereas they do not form in the ZnO-core/MgO (or other material)-shell nanorods with no faceted surfaces.

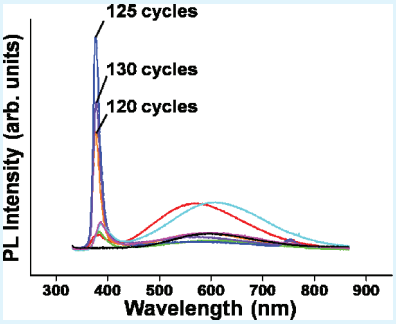

KEYWORDS: *MgO nanorods, ZnO sheath, photoluminescence, optical resonance cavity, short wavelength emission*

INTRODUCTION

The major advantage of the short-wavelength laser diodes (LD) is that they can impart higher information storage capacity to devices such as compact disk (CD) and digital video disk (DVD). For similar reasons laser printing systems also benefit from short-wavelength devices. White light-emitting diode (LED) illumination can also be realized by passing a short-wavelength LED through luminescent materials. On the other hand, LEDs based on one-dimensional (1D) nanostructures have many advantages over thin film-based LEDs. Considerably improved performance is expected from nanostructured active layers for light emission. 1D nanostructures can act as direct waveguides and favor light extraction without the use of lens and reflectors. In addition, the emission efficiency is boosted by the absence of nonradiative recombinations at the joint defects because the use of 1D nanostructures can avoid grain boundaries.[1] Therefore, it is very important to obtain ultraintense short-wavelength luminescence using 1D nanostructures.

A recent paper reported that intense emissions with a range of wavelengths over a wide spectral range, from ultraviolet to infrared light, might be possible by sheathing MgO nanorods with a semiconducting material with an optimal sheath thickness.[2] The paper showed that sheathing well-faceted MgO nanorods with TiO_2 (~20 nm) resulted in ultraintense blue-green luminescence (~220 times higher intensity than bare MgO nanorods). In addition, the paper hypothesized that an ultraintense short-wavelength emission could be obtained by sheathing MgO nanorods with a ZnO thin film ~17 nm thick. It is obvious that the enhancement of the short-wavelength emission, i.e. the near-band edge (NBE) emission and the suppression of the visible emission, i.e. the deep level (DL) emission of ZnO are desirable. However, there is no guarantee, in actuality, that the NBE emission, not the DL emission of ZnO is enhanced by this technique because the origin of the NBE emission of ZnO (excitons) differs from that of TiO_2 (deep levels) whereas the origin of the DL emission (deep levels) is basically the same as that of TiO_2. The aim of this paper is to verify the previously proposed hypothesis concerning the ultraintense short-wavelength emission from the MgO-core/ZnO-shell nanorods.

EXPERIMENTAL SECTION

MgO nanorods were synthesized on Au-coated Si (100) substrates in a quartz tube by the thermal evaporation of Mg_3N_2. Details of the MgO nanorod synthesis procedure are described elsewhere.[2] The prepared MgO nanorods were then transferred to an atomic layer deposition (ALD) chamber. The ZnO was deposited on the nanorods using the following method. The nanorods were coated with ZnO. Diethylzinc (DEZn) and H_2O were kept in bubblers at 0° and 10 °C, respectively. These source gases were alternatively fed into the chamber through separate inlet lines and nozzles. The typical pulse lengths were 0.15 s for DEZn, 0.2 s for H_2O and 3 s to purge the reactants. The substrate temperature and pressure in the chamber were 150 °C and 0.1 Torr, respectively. The photoluminescence measurements of the nanorod

Received: October 26, 2011
Accepted: February 6, 2012
Published: February 6, 2012

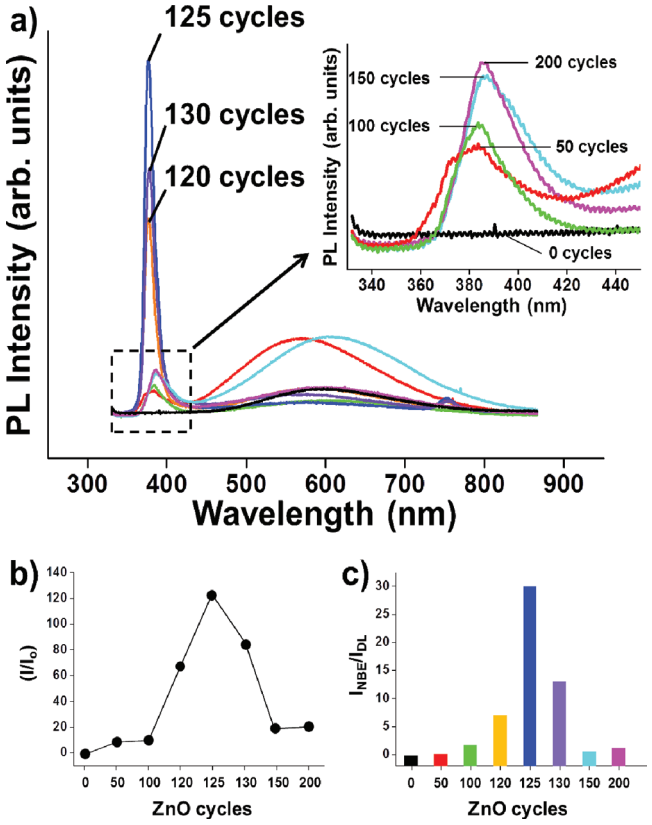

Figure 1. (a) PL spectra of the as-synthesized MgO-core/ZnO-shell nanorods for different ZnO sheathing times. (b) Plot of the normalized intensity of the major emission (I/I_0) of the core–shell nanorods as a function of the number of ALD cycles for ZnO deposition showing exceptionally intense emission for 125 ALD cycles, which is equivalent to a ZnO-shell layer thickness of ~17 nm. The PL intensity (I) was normalized to that of 0 ALD cycle (I_0). It is worthy of noting that I is the intensity of the NBE emission from MgO-core/ZnO-shell nanorods whereas I_0 is that of the DL emission from the MgO nanorods. (c) Plot of the intensity ratio of the NBE emission to the DL emission (I_{NBE}/I_{DL}) of the core–shell nanorods as a function of the number of ALD cycles for ZnO deposition.

samples were taken at room temperature using a PL spectrometer (SPEC-1403) with a He–Cd laser (325 nm, 55 MW) as the excitation source. The general surface morphology and crystallinity of the products were examined by scanning electron microscopy (SEM, Hitachi S-4200) and glancing angle (0.5°) X-ray diffraction (XRD, Rigaku DMAX 2500) with Cu–Kα radiation (λ = 0.1541 nm), respectively. A transmission electron microscope (TEM) instrument (Phillips CM-200) operated at 200 KV was used to examine the detailed microstructures of the products.

RESULTS AND DISCUSSION

A previous study[2] reported the optimal thickness of the ZnO shell layer in MgO-core/ZnO-shell nanorods for the maximum intensity of the near-ultraviolet emission from them. In the case of MgO-core/ZnO-shell nanorods, it was hypothesized that natural subwavelength optical resonance cavities form in the ZnO shell layer of each core–shell nanorod because the shell has dimensions larger than the Bohr radius but smaller than the optical wavelength.[3] For this core–shell nanorod system, considering the difference in refractive index between MgO and ZnO (1.736 for MgO, 2.0 for ZnO),[4] it was assumed that four resonance cavities form in the ZnO shell layer of each core–shell nanorod with a square cross-section, which is similar

Table 1. Comparison of the Intensity Ratios of the NBE Emission to the DL Emission (I_{NBE}/I_{DL}) for ZnO-Based Core–Shell 1D Nanostructures and MgO-Core/ZnO-Shell Nanorods[a]

core material	shell material	I_{NBE}/I_{DL}	ref
MgO	ZnO	30.0	present study
ZnO	SnO_2	2.6	7
ZnO	SnO_2	14.3	9
ZnO	ZnS	3.0	10
ZnO	MgO	3.5	12
ZnO	MgO	20.9	13
ZnO	MgO	0.7	14
ZnO	MgO	3.6	16
ZnO	Al_2O_3	4.0	17
ZnO	Ti	1.8	18
ZnO	Al	0.7	18
ZnO	Ni	0.3	18
ZnO	Au	2.0	18
ZnO	Au	16.4	19

[a]Only the reasonable data available from the corresponding references are listed. For example, cases where the I_{NBE}/I_{DL} value is infinite because I_{DL} = 0 in spite of low I_{NBE} values are excluded in this list.

to the MgO-core/TiO_2-shell nanorod system.[2] The cavity length d in a Fabry–Perot cavity[5] can be expressed as

$$d = \frac{m_c \lambda}{2n} \quad (1)$$

where λ and n are the wavelength of the light and the refractive index of the semiconductor, respectively, and m_c is the cavity order, which is a measure of the resonance modes in the cavity. Assuming that m_c = 1 because the cavity length is quite short, the cavity length for optical resonance was calculated to be ~94 nm by placing $\lambda \approx$ 380 nm and $n \approx$ 2.0 (the refractive index of ZnO) into the above equation. Therefore, the predicted thickness of the ZnO shell layer was ~17 nm for the MgO nanorods with an average width of 60 nm considering the refractive index of ZnO (~2.0). In addition, it was reported that it was essential to form shell layers with a good thickness uniformity as well as an optimal thickness to obtain the maximum oscillator strength effect. Therefore, a chemical vapor deposition technique such as ALD or metal organic chemical vapor deposition is desirable to produce uniform ZnO sheaths.

Figure 1a shows the room-temperature PL spectra of the as-synthesized MgO-core/ZnO-shell nanorods. In the enlarged photoluminescence spectra (inset), the 0 ALD cycle corresponds to the as-synthesized MgO nanorods. The photoluminescence spectrum of the as-synthesized MgO nanorods showed a broad emission band centered at approximately 595 nm in the yellow region. On the other hand, the ZnO-sheathed MgO nanorods showed two characteristic emission bands: a sharp near-band edge emission band centered at approximately 380 nm in the near-ultraviolet region and a broad deep level emission band centered in a range, 560–610 nm. These two bands are assumed to originate from the ZnO shell layer rather than from the MgO core because the wavelengths of the two major emission peaks match those of the near-band edge and deep level emissions from ZnO very well. Figure 1b shows the PL intensities of the core–shell nanorods for different numbers of ALD cycles, i.e., different shell layer thicknesses, relative to that of the as-synthesized MgO nanorods (I/I_0). The highest PL intensity was obtained at 125 ALD cycles, which

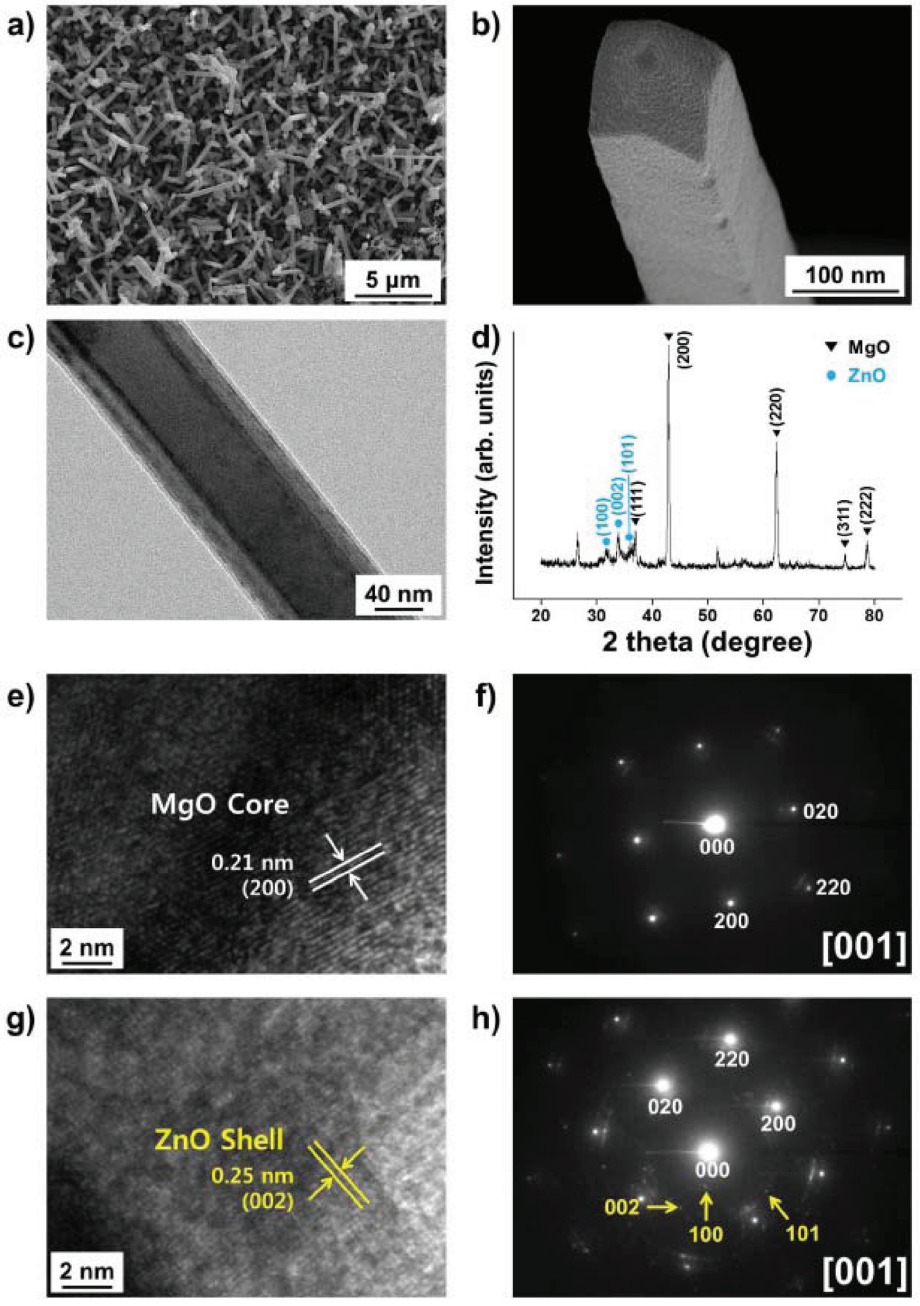

Figure 2. SEM and TEM images and corresponding electron diffraction patterns of the MgO-core/ZnO-shell nanorods (125 ALD cycles). (a) SEM image of the MgO-core/ZnO-shell nanorods synthesized using a two-step process: thermal evaporation of Mg_3N_2 and ALD of ZnO. (b) Enlarged SEM image of a typical core−shell nanorod showing a square cross-section and the faceted surfaces perpendicular to it. (c) Low-magnification TEM image of a typical core−shell nanorod showing the excellent thickness uniformity of the shell layer. (d) XRD pattern of a typical MgO-core/ZnO-shell nanorod. (e) HRTEM image of the core layer. (f) SAED corresponding to the HRTEM image in (e), indicating that the MgO core is a single crystal with an fcc structure. (g) HRTEM image of the shell layer. (h) SAED pattern corresponding to the HRTEM image in (g), indicating that the ZnO shell layer is primitive hexagonal-structured polycrystalline. The Miller indices typed in yellow represent the reflections from ZnO, whereas those typed in white represent the reflections from MgO.

corresponds to a shell layer thickness of ~17 nm. This result is in good agreement with the hypothesis in a previous paper.[2] The intensity of the ultraviolet emission of the MgO-core/ZnO-shell nanorods for 125 cycles (corresponding to a ZnO shell layer thickness of ~17 nm) is ~120 times higher than that of the yellow emission from the unsheathed MgO nanorods (0 cycle). Figure 1c shows that the intensity ratio of near-band edge emission to deep level emission, I_{NBE}/I_{DL}, is as high as ~30 for 125 cycles whereas the I_{NBE}/I_{DL} ratio of bare MgO nanorods is 0. A high intensity ratio, I_{NBE}/I_{DL}, rather than a high I/I_0 ratio is essential for realizing ZnO-based optical and optoelectronic devices with high performance. The wavelengths of the two major emission peaks of the core−shell nanorods are in good agreement with those of the near-band edge and deep level emissions from ZnO and that the near-band edge emission intensity depends strongly on the ZnO layer thickness. Therefore, it was hypothesized that the near-ultraviolet emission from the core−shell nanorods is characteristic of the

dx.doi.org/10.1021/am2014794 | ACS Appl. Mater. Interfaces 2012, 4, 1262−1266

ZnO shell, not the MgO core, even if the ZnO shells are much thinner than the MgO cores. The ultraintense near-ultraviolet emission from the MgO-core/ZnO-shell nanorods might be due to the transfer of photogenerated electrons from the MgO core to the ZnO shell[6] and an oscillator strength effect due to optical resonance cavity formation as was described in depth in a previous paper.[2]

Enhanced near-band edge emission can also be obtained by sheathing the ZnO 1D nanostructures with MgO instead of sheathing the MgO nanorods with ZnO. Indeed, sheathing ZnO 1D nanostructures with other materials to enhance the near-band edge emission and simultaneously to suppress the deep level emission of 1D ZnO nanostructures has been studied extensively.[7−23] The sheath materials include ceramics (e.g., SnO_2,[7−9] ZnS,[10,11] MgO,[12−15] and Al_2O_3[16]), metals (e.g., Ti,[17] Al,[17] Ni,[17] Au,[17,18] and Ag,[19] Pt,[20]) and polymers (e.g., polymethyl methacrylate[21] and polyaniline[22]). On the other hand, Table 1 obviously shows that this PL intensity enhancement by sheathing ZnO 1D nanostructures with other material such as MgO is not as significant as that by sheathing MgO nanorods with ZnO. The enhancement in I_{NBE}/I_{DL} ratio by sheathing ZnO 1D nanostructures with MgO was reported to be mainly due to the quantum confinement of the photogenerated carriers inside the ZnO core, which is caused by the larger energy band gap of the MgO shell than that of the ZnO core.[12,13] The relatively high I_{NBE}/I_{DL} ratio values for the ZnO 1D nanostructure-base core−shell structures in refs 9, 13, and 19 in Table 1 suggest that a giant oscillator strength effect due to optical resonance cavity formation might also have been obtained in those nanostructures. However, MgO-core/ZnO-shell nanorods showed a far higher I_{NBE}/I_{DL} ratio than the ZnO 1D nanostructure-base core−shell structures. It is not clear why the former showed a higher I_{NBE}/I_{DL} ratio than the latter at present, but we surmise that it is attributed to the following two factors:

(1) MgO 1D nanostructures have more faceted morphologies for easier optical resonance cavity formation than ZnO 1D nanostructures
(2) The emission from the ZnO core is partly absorbed by the shell layer in the latter core before it reaches our eyes whereas the emission from the ZnO shell is not absorbed by the MgO core layer.

Figure 2a shows the SEM images of the MgO-core/ZnO-shell nanorods synthesized by the thermal evaporation of Mg_3N_2 powders at 900 °C for 1 h in an oxidizing atmosphere and the ALD of ZnO at 150 °C for 125 cycles. SEM observation of the core−shell nanorods revealed widths ranging from 50 to 200 nm and lengths ranging from 3 to 5 μm. Figure 2b clearly displays the geometrical configuration of a typical core−shell nanorod with a square cross-section and faceted surfaces. Low-magnification TEM (Figure 2c) revealed excellent thickness uniformity of the ZnO shell layer formed on an MgO nanorod by ALD even if the shell layer on the left side appeared to be somewhat thicker than that on the right side. The XRD pattern of the as-synthesized MgO-core/ZnO-shell nanorods (Figure 2d) showed that both the ZnO shells and MgO cores are crystalline. The (100), (002), and (101) reflection peaks of ZnO were observed alongside the reflection peaks of MgO. The heights of the ZnO reflection peaks were much smaller than those of the MgO reflection peaks possibly because the ZnO shell layers are much thinner than the MgO cores. The local high-resolution TEM image in Figure 2e shows the microstructure of the MgO core in a typical core−shell nanorod. The fringe pattern in the high-resolution TEM indicates the MgO core to be a single crystal. The resolved spacing between two parallel neighboring fringes (Figure 2e) was 0.21 nm, which matches well that of the {200} lattice plane family of a face-centered cubic (fcc) ($Fm3m$)-structured MgO with a lattice parameter of a = 0.4213 nm (JCPDS No. 04−0829). The corresponding selected area electron diffraction pattern (Figure 2f) clearly exhibits strong reflections from the fcc-structured MgO. A fringe pattern was also observed in the HRTEM of the shell region (Figure 2g), indicating that the ZnO shell to also be of single crystal nature locally even though the overall structure of the ZnO shell is polycrystalline. The resolved spacing between two parallel neighboring fringes in the shell region was 0.25 nm, which is in good agreement with those of the {002} lattice plane families of primitive hexagonal-structured ZnO with lattice parameters of a = 0.3241 and c = 0.5187 nm (JCPDS No. 79−0205). The selected area electron diffraction pattern recorded from the shell layer (Figure 2h) showed a set of spotty pattern and a set of ring pattern overlapping each other. In addition to the strong spotty reflections corresponding to fcc-structured single crystal MgO, dim {100}, {002}, and {101} spotty reflections on concentric circles from hexagonal-structured polycrystalline ZnO could be identified. The reflections from the ZnO shell layer were much weaker than those from the MgO core because the shell layer is much thinner than the core.

CONCLUSIONS

In summary, this study confirmed the previous hypothesis that ultraintense short-wavelength emission could be obtained by sheathing MgO nanorods with a ∼17 nm ZnO thin film. The I_{NBE}/I_{DL} ratio of the MgO-core/ZnO-shell nanorods was as high as ∼30 for 125 ALD cycles of ZnO deposition (corresponding to a ZnO shell layer thickness of ∼17 nm), whereas the I_{NBE}/I_{DL} ratio of the bare-MgO nanorods was 0. This near- band edge emission intensity enhancement by sheathing the MgO nanorods with ZnO is by far more significant than those by sheathing the ZnO nanorods with other materials including MgO. This is because subwavelength optical resonance cavities form in the MgO-core/ZnO-shell nanorods with faceted surfaces, whereas they do not form in the ZnO-core/MgO-shell nanorods with no faceted surfaces. We believe that this finding will make a significant contribution to the fabrication of nanoscale short wavelength light emitting devices such as LEDs, laser diodes, and building blocks for nanoscale electronic and optoelectronic devices of high performance.

AUTHOR INFORMATION

Corresponding Author

*E-mail: cmlee@inha.ac.kr.

Notes

The authors declare no competing financial interest.

ACKNOWLEDGMENTS

This study was supported by the Korea Research Foundation (KRF) through 'the 2007 National Research Lab Program'.

REFERENCES

(1) Lupan, O.; Pauporte, T.; Viana, B. *Adv. Mater.* **2010**, *22*, 3298−3302.
(2) Jin, C.; Kim, H.; Lee, W. I.; Lee, C. *Adv. Mater.* **2011**, *23*, 1982−1987.

(3) Yang, P.; Yang, H.; Mao, S.; Russo, R.; Johnson, J.; Saykally, R.; Morris, N.; Pham, J.; He, R.; Choi, H.-J. *Adv. Funct. Mater.* **2002**, *12*, 323−331.
(4) Lide, D. R. In *CRC Handbook of Chemistry and Physics* 80th ed.; CRC Press: Boca Raton, FL, 1999.
(5) Delbeke, D.; Bockstaele, R.; Bienestman, P.; Baets, R.; Benisty, H. *IEEE J. Sel. Top. Quantum Electron.* **2002**, *8*, 189−206.
(6) Özgür, Ü.; Alivov, Ya. I.; Liu, C.; Teke, A.; Reshchikov, M. A.; Doğan, S.; Avrutin, V.; Cho, S.-J.; Morkoç, H. *J. Appl. Phys.* **2005**, *98*, 041301.
(7) Kuang, Q.; Jiang, Z.-Y.; Xie, Z.-X.; Lin, S.-C.; Lin, Z.-W.; Xie, S.-Y.; Huang, R.-B.; Zheng, L.-S. *J. Am. Chem. Soc.* **2005**, *127*, 11777−11784.
(8) Yu, W. D.; Li, X. M.; Gao, X. D. *Nanotechnology* **2005**, *16*, 2770−2774.
(9) Shi, L.; Xu, Y.; Hark, S.; Liu, Y.; Wang, S.; Peng, L.; Wong, K.; Li, Q. *Nano Lett.* **2007**, *7*, 3559−3563.
(10) Li, J.; Zhao, D.; Meng, X.; Zhang, Z.; Zhang, J.; Shen, D.; Lu, Y.; Fan, X. *J. Phys. Chem. B* **2006**, *110*, 14685−14687.
(11) Murphy, M. W.; Zhou, X. T.; Ko, J. Y. P.; Zhou, J. G.; Heigl, F.; Sham, T. K. *J. Chem. Phys.* **2009**, *130*, 084707.
(12) Jin, C.; Kim, H.; Hong, C.; Lee, J.; Lee, C. *Curr. Appl. Phys.* **2011**, *11*, S60−S64.
(13) Fu, Z.; Dong, W.; Yang, B.; Wang, Z.; Yang, Y.; Yan, H.; Zhang, S.; Zuo, J.; Ma, M.; Liu, X. *Sol. State Comm.* **2006**, *138*, 179−183.
(14) Shimpi, P.; Gao, P. X.; Goberman, D. G.; Ding, Y. *Nanotechnology* **2009**, *20*, 125608.
(15) Plank, N.O. V.; Snaith, H. J.; Ducati, C.; Bendall, J. S.; Schmidt-Mende, I.; Welland, M. E. *Nanotechnology* **2008**, *19*, 465603.
(16) Richter, J.-P.; Voss, T.; Kim, D. S.; Scholz, R.; Zacharias, M. *Nanotechnology* **2008**, *19*, 305202.
(17) Fang, Y. J.; Sha, J.; Wang, Z. L.; Wan, Y. T.; Xia, W. W.; Wang, Y. W. *Appl. Phys. Lett.* **2011**, *98*, 033103.
(18) Li, X.; Zhang, Y.; Ren, X. *Opt. Express* **2009**, *17*, 8735−8740.
(19) Abiyasa, A. P.; Yu, S. F.; Lau, S. P.; Leong, E. P.; Yang, H. Y. *Appl. Phys. Lett.* **2007**, *90*, 231106.
(20) Lin, J. M.; Lin, H. Y.; Cheng, C. L.; Chen, Y. F. *Nanotechnology* **2006**, *17*, 4391−4394.
(21) Liu, K. W.; Chen, R.; Xing, G. Z.; Wu, T.; Sun, H. D. *Appl. Phys. Lett.* **2010**, *96*, 023111.
(22) Zheng, Z. X.; XI, Y. Y.; Dong, P.; Huang, H. G.; Zhou, J. Z.; Wu, L. L.; Lin, Z. H. *Phys. Chem. Comm.* **2002**, *5*, 63.
(23) Yu, K.; Zhang, T.; Xu, R.; Jiang, D.; Luo, L.; Li, Q.; Zhu, Z.; Lu, W. *Solid State Commun.* **2005**, *133*, 43−47.